Thermomagnetic convection of magnetic fluids in a cylindrical geometry

Adrian Lange[a)]

Institut für Theoretische Physik, Universität Magdeburg, Postfach 4120, D-39016 Magdeburg, Germany

The thermomagnetic convection of magnetic fluids in a cylindrical geometry subjected to a homogeneous magnetic field is studied. The study is motivated by a novel thermal instability [W. Luo *et al.*, Phys. Rev. Lett. **82**, 4134 (1999)]. As model system a composite cylinder with inner heating is considered which reflects the symmetry of the experimentally setup. The general condition for the existence of a potentially unstable stratification in the magnetic fluid is derived. Within a linear stability analysis the critical external induction for the onset of thermomagnetic convection is determined for dilute and nondilute magnetic fluids. The difference between both thresholds allows to test experimentally whether a test sample is a dilute fluid or not. © *2002 American Institute of Physics.* [DOI: 10.1063/1.1480264]

I. INTRODUCTION

Magnetic fluids (MFs) are superparamagnetic fluids formed by a stable colloidal suspension of ferromagnetic nanoparticles dispersed in a carrier liquid.[1] The behavior of MFs is characterized by the complex interaction of their hydrodynamic and magnetic properties with external forces. For the phenomenon of thermomagnetic convection these forces are a temperature gradient and a magnetic field. Most studies consider the geometry of a horizontal layer which is simultaneously subjected to a vertical temperature gradient and either to a constant vertical magnetic field[2–4] or to a vertical magnetic field with a constant gradient.[5] Studies for a cylindrical geometry are few[6,7] and focus on the thermomagnetic convection under microgravity.[8]

The present analysis of thermomagnetic convection in a cylindrical geometry is motivated by a recently observed novel convective instability. In Refs. 9 and 10 a horizontal layer of MF between two glass plates is locally heated by a focused laser beam. It passes perpendicularly through the layer in the presence of a homogeneous vertical magnetic field. The absorption of the light by the fluid generates a temperature gradient and subsequently a refractive index gradient. This gradient is optically equivalent to a diverging lens, leading to an enhancement of the beam divergence. As result, a stationary diffraction pattern of concentric rings is observed for zero magnetic field. Above a certain threshold of the magnetic field, the circular rings are replaced by polygonally shaped patterns which switch among different shapes alternatively. Based on *numerics* it was stated that the characteristic time scales for mass and thermal diffusion are equal.[9] Thus thermal conduction and thermal diffusion contribute equally to the formation of the diverging lens. The polygonally shaped diffraction patterns were interpreted as "fingerprints" of vertical convection columns.[10]

Both claims are controversial due to the following reasons. An analysis of the *physical quantities* reveals that both characteristic time scales are several orders of magnitude apart (below and Ref. 11). Direct spatial temperature measurements[12] and independent measurements of all relevant material parameters for organic dispersions[13] showed that the ring pattern is essentially caused by the temperature contribution and not by the concentration contribution. The determination of the relevant time scales confirmed that the experiment is dominated by the characteristic time for convection. Presently there is no sound theoretical description for the dependence of the size of the outmost of the concentric rings on the laser power (see Fig. 2 in Ref. 13).

A major hindrance of the studied system in Refs. 9 and 10 is that it is almost impossible to gain information about the spatial distribution of temperature and concentration inside the MF layer. Due to the lack of sound internal information many hypotheses can be brought forward to explain the experimental results. Among them is the recent discussion whether the shape instability of a hot nonmagnetic bubble surrounded by MF can be accounted for the observed phenomena.[14,15]

This situation motivates the present work in which a model system is studied which reflects the essentials of the experimental setup. These are the axis-symmetry of the heating and the finite height and width of the layer. The aim is to determine the necessary conditions and the critical magnetic inductions for the appearance of axial convection columns. Thus the focus is on the general requirements for thermomagnetic convection in an axis-symmetric heated system.

This paper is organized as follows: The system and the relevant equations of the problem as well as the condition for a potentially unstable stratification in the fluid are displayed in the next section. Based on a linear stability analysis (Sec. III), the results are presented and discussed in Sec. IV. In the final section, the results are summarized.

II. MODEL AND EQUATIONS

The model system is given by a composite, circular cylinder of height h which consists of three parts. The inner

---

[a)]Author to whom correspondence should be addressed. Fax: +49-391-6711205; electronic mail: adrian.lange@physik.uni-magdeburg.de
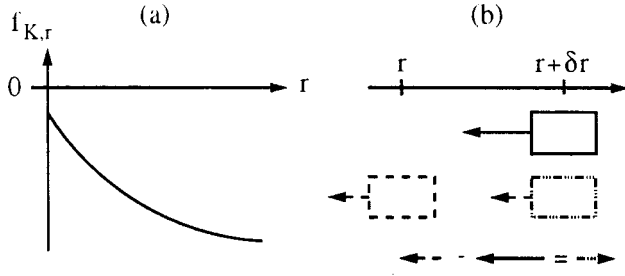
FIG. 1. Required destabilizing force profile of the radial component of the magnetic force density $f_{K,r}$ for inner heating (a). A fluid volume at the distance $r+\delta r$ [solid rectangle, (b)] experiences a larger force than a fluid volume at the distance r [dashed rectangle, (b)]. Moving the latter volume from r to $r+\delta r$ [dot–dashed rectangle, (b)] results in an effective force which points in the direction of the displacement [dot–dashed arrow, (b)].

cylinder of radius R_1, constant temperature T_1, and constant susceptibility $\chi(T_1)$ is surrounded by a middle cylinder of radius R_2. In the gap R_2-R_1 the temperature decreases to $T_0 < T_1$ and consequently χ is a spatially varying quantity, $\chi = \chi[T(r)]$. The outer cylinder has the radius R_{out}, where in the region $R_{\text{out}}-R_2$ the constant temperature T_0 and constant susceptibility $\chi(T_0)$ is present. The whole system is subjected to a homogeneous vertical magnetic field and its effective susceptibility is given by

$$\chi_{\text{eff}} = \frac{1}{R_{\text{out}}}\left(R_1 \chi(T_1) + (R_2 - R_1) \right.$$

$$\left. \times \int_{R_1}^{R_2} dr\,\chi[T(r)] + (R_{\text{out}} - R_2)\chi(T_0) \right). \quad (1)$$

In the presence of a uniform external magnetic induction $\mathbf{B}_{\text{ext}}$, the internal field in the gap is given by $\mathbf{H}_{\text{int}} = \mathbf{B}_{\text{ext}}/[\mu_0(1+N\chi)]$. The susceptibility of the MF is $\chi = \chi_L(1+\beta_1\chi_L)$, where χ_L is the susceptibility according to Langevins theory which assumes noninteracting particles. Higher-order terms in χ_L are included in order to determine the magnetic (or Kelvin) force density beyond the dilute limit $\chi = \chi_L$. The coefficient β_1 was determined in different microscopic models[16–18] which all provide the same value $\beta_1 = 1/3$. The demagnetization factor N accounts for the finite size of the composite cylinder and is a function of the height-to-diameter ratio $\gamma = h/(2R_{\text{out}})$ and the effective susceptibility χ_{eff}.[19] The Kelvin force follows then as[20]

$$\mathbf{f}_K = -\frac{B_{\text{ext}}^2}{\mu_0} F_{\chi_L} \frac{\text{grad}\,\chi_L}{\chi_L}, \quad (2)$$

where

$$F_{\chi_L} = \frac{\chi_L^2\{N + \beta_1[3N\chi_L(1+\beta_1\chi_L) - 1]\}}{(1+N\chi)^3}. \quad (3)$$

Considering MFs as binary mixtures, it is necessary to evaluate the influence of temperature and concentration on pattern phenomena by analyzing the corresponding time scales. These are the characteristic time for convection $t_c = L_c^2/\kappa$ and for mass diffusion $t_d = L_d^2/D$, where L_c (L_d) is the typical length for convection (diffusion), κ the thermal

diffusivity, and D the mass diffusion coefficient. Using the data given in Refs. 1 and 9, one gets $\kappa \sim 4\times 10^{-8}$ m^2 s^{-1} and $D \sim 8\times 10^{-12}$ m^2 s^{-1}. Except in special designed geometries as in Ref. 21, where $L_c \gg L_d$, the characteristic time for diffusion is of three orders of magnitude larger than the characteristic time for convection. Since in our model both length scales are equal to the gap width $R_2 - R_1$, diffusion phenomena can be neglected.

The system is governed by the equation of continuity, the Navier–Stokes equations, and the equation of heat conduction for the MF which are in nondimensional form

$$\text{div}\,\bar{\mathbf{v}} = 0, \quad (4)$$

$$\frac{\partial \bar{\mathbf{v}}}{\partial \bar{t}} + (\bar{\mathbf{v}}\,\text{grad})\bar{\mathbf{v}} = \mathcal{P}(-\text{grad}\,\bar{p} + \Delta\bar{\mathbf{v}}) + \mathcal{M}F_{\chi_L}\frac{\text{grad}\,\bar{T}}{\bar{T}}, \quad (5)$$

$$\frac{\partial \bar{T}}{\partial \bar{t}} + (\bar{\mathbf{v}}\,\text{grad})\bar{T} = \Delta\bar{T}, \quad (6)$$

where the Prandtl number $\mathcal{P} = \nu/\kappa$ characterizes the fluid and the magnetization number $\mathcal{M} = B_{\text{ext}}^2(R_2-R_1)^2/(\mu_0\rho\kappa^2)$ tunes the external excitation. Denoting ν as kinematic viscosity, the velocity $\mathbf{v} = (u,v)$ is scaled with $\kappa/(R_2-R_1)$, time with $(R_2-R_1)^2/\kappa$, temperature with (T_1-T_0), and pressure p with $\rho\kappa\nu/(R_2-R_1)^2$. Δ and grad are the corresponding differential operators in the plane cylindrical coordinates $\bar{r}$ and ϕ. Rigid boundary conditions are assumed for the velocity at the inner and outer radius of the gap, $\bar{u} = \partial_{\bar{r}}\bar{u} = 0$ at $\bar{r} = \eta/(1-\eta)$ and $\bar{r} = 1/(1-\eta)$, where the radii ratio is given by $\eta = R_1/R_2$. The temperature is assumed to be constant at each boundary, $\bar{T}(\bar{r} = \eta/(1-\eta)) = \bar{T}_1$ and $\bar{T}(\bar{r} = 1/(1-\eta)) = \bar{T}_0$.

Since the Kelvin force is the only destabilizing force present in the system, one has to determine which profile leads to a potentially unstable stratification in the fluid. For heating at the inner radius, the required profile is given in Fig. 1(a): The r-component of the Kelvin force density has to act inwards and its absolute value increases monotonically outward. With such a profile a fluid volume at the distance $r+\delta r$ [solid rectangle in Fig. 1(b)] experiences a larger force towards the center compared to a fluid volume at the distance r (dashed rectangle). Moving the latter fluid volume from r to $r+\delta r$ (dot–dashed rectangle) results in an effective force which points in the direction of the displacement [indicated symbolically by the subtraction of the arrows in Fig. 1(b) bottom]. This force may enhance small displacements of warmer fluid volumes towards cooler regions and thus making the stratification potentially unstable.

The above argument has to be tested for the quiescent conductive state which is given by $\bar{\mathbf{v}}_G = 0$ and $\bar{T}_G = \bar{T}_0 + (\bar{T}_1 - \bar{T}_0)\ln[\bar{r}(1-\eta)]/\ln\eta$. Applying the condition for a destabilizing force profile to the r-component of the Kelvin force density in Eq. (2) leads to the condition

$$\frac{\partial}{\partial \bar{r}} f_{K,\bar{r}} = -\mathcal{M}\left(\frac{\partial_{\bar{r}}\bar{T}}{\bar{T}}\right)^2 \frac{\partial(\chi_L F_{\chi_L})}{\partial\chi_L} + \mathcal{M}F_{\chi_L}\frac{\partial_{\bar{r}}^2\bar{T}}{\bar{T}}$$

$$< 0 \quad \text{for all}\ \ \bar{r} \in [\eta/(1-\eta), 1/(1-\eta)]. \quad (7)$$

Phys. Fluids, Vol. 14, No. 7, July 2002

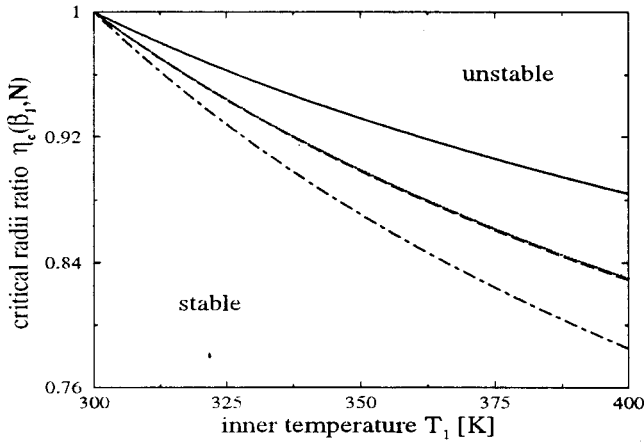Thermomagnetic convection of magnetic fluids 2061

FIG. 2. Region of potentially unstable and stable force profiles for a fixed outer temperature of $T_0 = 300$ K and $\chi_L = 3$. The four different sets are $\beta_1 = 0$, $N = 1$ (long-dashed line), $\beta_1 = 0$, $N = 0.7$ (dot–dashed line), $\beta_1 = 1/3$, $N = 1$ (solid line), and $\beta_1 = 1/3$, $N = 0.7$ (dotted line), where the first and last one practically coincide.

Since $\partial_{\bar{r}} f_{K,\bar{r}}$ is a monotonously decreasing function of $\bar{r}$, it is sufficient if $\partial_{\bar{r}} f_{K,\bar{r}} < 0$ at $\bar{r} = \eta/(1-\eta)$ in order to fulfill the condition (7). Depending on the temperatures $\bar{T}_1$ and $\bar{T}_0$, the Langevin susceptibility χ_L, the demagnetization factor N, and β_1 the condition (7) entails that the radii ratio η has to be larger than a critical value. For realistic temperatures T_1 above a room temperature of $T_0 = 300$ K, it becomes clear that this condition is met only in a narrow gap (see Fig. 2). This is plausible because the nonlinear temperature profile $\bar{T}_G \sim \ln[\bar{r}(1-\eta)]$ can be well approximated in a small gap by a linear profile which always satisfies the requirement (7) if $\beta_1 = 0$.

III. LINEAR STABILITY ANALYSIS

Exploiting the smallness of the gap, in the linear stability analysis terms as $\partial_{\bar{r}}(\partial_{\bar{r}} + 1/\bar{r})$ are approximated by $\partial_{\bar{z}}^2$ and the new variable $\zeta = \bar{r} - \eta/(1-\eta)$ is introduced. All small disturbances from the ground state are decomposed into normal modes, i.e., into components of the form $[\bar{u}, \bar{p}, \bar{T}] = e^{n\bar{t}} \cos(l\phi)[\bar{u}(\zeta), \bar{p}(\zeta), \bar{T}(\zeta)]$ and $\bar{v} = e^{n\bar{t}} \sin(l\phi)\bar{v}(\zeta)$, respectively. The nondimensional growth rate is denoted by n and l is the azimuthal wave number. For marginal stability, $n \equiv 0$, the differential equations to solve are

$$\left(\frac{\partial^2}{\partial\zeta^2} - \alpha^2\right)^2 \bar{u} - \frac{\alpha^2}{l^2}\left(\frac{\partial^2}{\partial\zeta^2} - \alpha^2\right)\bar{u}$$

$$= -\alpha^2 \frac{\mathcal{M}}{\mathcal{P}} f_{\chi_L} \frac{\bar{T}}{\bar{T}_G^2} \frac{\partial \bar{T}_G}{\partial\zeta}, \tag{8}$$

$$\left(\frac{\partial^2}{\partial\zeta^2} - \alpha^2\right)\bar{T} = \bar{u}(\bar{T}_0 - \bar{T}_1), \tag{9}$$

where $\alpha = (1-\eta)l/\eta$ and

TABLE I. Critical external induction B_c in dependence of the order of approximation for $N = 1$.

T_1 [K]	β_1	B_c [T]			
		$K = 1$	$K = 2$	$K = 3$	$K = 4$
306	0	8.2527	8.2527	8.2502	8.2502
	1/3	5.1952	5.1952	5.1937	5.1937
320	0	0.4674	0.4674	0.4673	0.4673
	1/3	0.2942	0.2942	0.2942	0.2942
340	0	0.1178	0.1178	0.1177	0.1177
	1/3	0.074 13	0.074 13	0.074 11	0.074 11
370	0	0.042 30	0.042 29	0.042 28	0.042 28
	1/3	0.026 63	0.026 62	0.026 62	0.026 62

$$f_{\chi_L} = -\chi_L \frac{\partial F_{\chi_L}}{\partial \chi_L}$$

$$= \frac{\chi_L^2}{(1+N\chi)^4}[6N^2\beta_1^2\chi_L^3(1+\beta_1\chi_L)$$

$$+ 4N\chi_L^2\beta_1(N-4\beta_1) + \chi_L(N-10\beta_1) + 2\beta_1$$

$$- 2N]. \tag{10}$$

In order to satisfy the four boundary conditions $\bar{u} = \partial_\zeta \bar{u} = 0$ at $\zeta = 0, 1$, the ansatz

$$\bar{u}(\zeta) = \sum_{m=1}^{K} P_m[\sinh(a\zeta) + B_m\cosh(a\zeta)$$

$$+ C_m\sin(b\zeta) + D_m\cos(b\zeta)], \tag{11}$$

with $a = \sqrt{q_m^2 + \alpha^2}$ and $b = \sqrt{q_m^2 - \alpha^2}$ is chosen. q_m is a root of a transcendental equation and the constants B_m, C_m, and D_m are determined by the boundary conditions (for details see Ref. 22). With Eq. (11) the solution of Eq. (9) reads $\bar{T}(\zeta) = \Sigma_{m=1}^{K} P_m[T_m(\zeta) + C_1 e^{\alpha\zeta} + C_2 e^{-\alpha\zeta}]$. $T_m(\zeta)$ is the solution of the inhomogeneous equation (due to its lengths not given here) and the constants C_1 and C_2 are determined by the boundary conditions $\bar{T} = 0$ at $\zeta = 0, 1$. Using Eq. (11) and the solution for $\bar{T}(\zeta)$, Eq. (8) can be approximately solved by the Galerkin method. Due to the good convergence, all presented results are based on the third approximation (see Table I). For the calculations fluid parameters of EMG 901 are used: $\rho = 1.53 \times 10^3$ kg m^{-3}, $v = 6.54 \times 10^{-6}$ m^2 s^{-1}, $\chi_L = 3$, and $\kappa = 4.2 \times 10^{-8}$ m^2 s^{-1}.[23] The temperature at the outer radius of the gap $R_2 = 1$ cm is fixed at $T_0 = 300$ K. The height of the composite cylinder is given by $h = 1$ cm and the inner radius by $\eta = 1.01 \eta_c(\beta_1 = 1/3, N = 1)$. The choice of $\eta_c(\beta_1 = 1/3, N = 1)$ (solid line in Fig. 2) ensures that for all following parameter sets the condition (7) is fulfilled.

IV. RESULTS AND DISCUSSION

Solving Eq. (8) with the Galerkin method and subsequently minimization with respect to the azimuthal wave number determines the critical external induction B_c and the corresponding wave number l_c (Figs. 3 and 4). Four different parameter sets were chosen: A dilute ($\beta_1 = 0$) and a nondilute ($\beta_1 = 1/3$) MF with $R_{\text{out}} = \infty$ ($N = 1$) and $R_{\text{out}} \simeq 3.33$ cm, respectively. The demagnetization factor N for
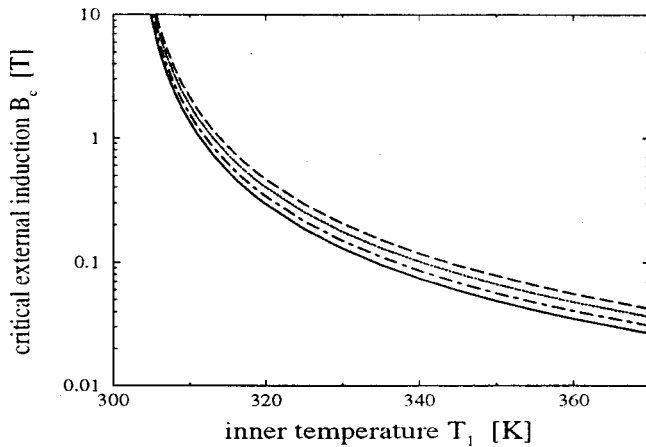
FIG. 3. Critical external induction B_c vs inner temperature T_1 for a room temperature of $T_0=300$ K. For a horizontally infinitely extended layer, i.e., $R_{\text{out}}=\infty$, the inclusion of a quadratic term in the susceptibility with $\beta_1=1/3$ (solid line) results in a lower threshold for the onset of convection than in the dilute case, $\beta_1=0$ (long-dashed line). Contrary for $R_{\text{out}}\simeq3.33$ cm, the critical induction for the dilute fluid (dot–dashed line) is lower than for the nondilute fluid (dotted line). The fluid parameters of the magnetic fluid EMG 901 and the size of the cylinder are given in the text.

the resulting height-to-diameter ratio $\gamma=0.15$ and the effective susceptibility χ_{eff} of the composite cylinder accordingly to Eq. (1) is taken from the data given in Ref. 19.

Decreasing the temperature difference from $\Delta T=70$ K to $\Delta T=4$ K causes a dramatic increase in the critical induction of nearly three orders of magnitude (Fig. 3). With decreasing temperature difference the critical radii ratio grows, i.e., the allowed gap becomes more narrow. Since the convection rolls prefer the same length scale in r and ϕ-direction, much more rolls have to be driven in a very small gap. The energy for this effort comes from the external induction which is why it amplifies drastically for small ΔT (Fig. 3).

Whereas the critical azimuthal wave number l_c is independent of $\chi(\chi_L)$ and N (Fig. 4), the critical induction varies.
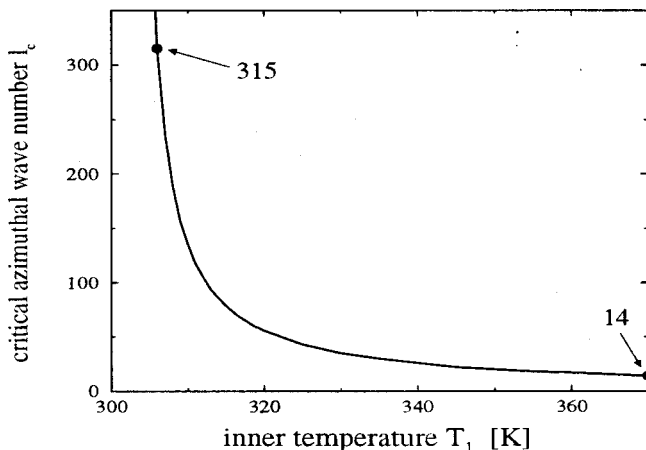
FIG. 4. Critical azimuthal wave number l_c vs inner temperature T_1 for $T_0=300$ K. With decreasing temperature difference the wave number, i.e., the number of convection rolls, increases dramatically from $l_c=14$ for $\Delta T=70$ K to $l_c=315$ for $\Delta T=6$ K ($\bullet$).
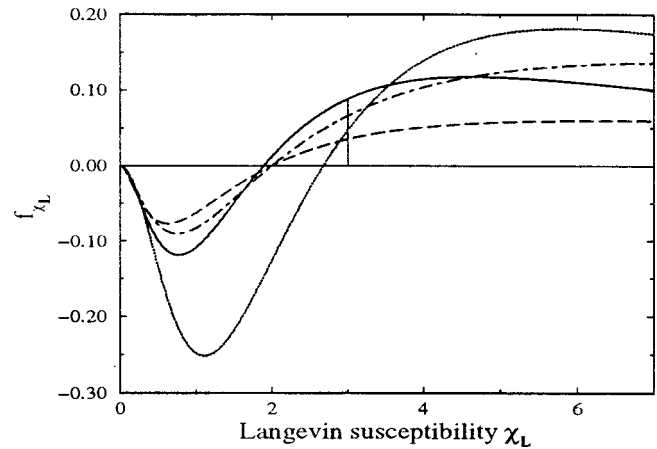
FIG. 5. f_{χ_L}, a measure for the strength of the magnetic force, versus the Langevin susceptibility χ_L. The four different sets are $\beta_1=0$, $N=1$ (long-dashed line), $\beta_1=1/3$, $N=1$ (solid line), $\beta_1=0$, $N(\gamma=0.15,\chi_{\text{eff}})$ (dot–dashed line), and $\beta_1=1/3$, $N(\gamma=0.15,\chi_{\text{eff}})$ (dotted line). The vertical solid line at $\chi_L=3$ is a guide for the eye.

First the two thresholds for the case of an infinitely extended layer, $R_{\text{out}}=\infty$, are compared. The inclusion of a quadratic term in the susceptibility with $\beta_1=1/3$ results in a lower threshold for the onset of convection than in the dilute case $\beta_1=0$ (solid and long-dashed line in Fig. 3). The difference between the thresholds is nearly the same value, $B_c(\beta_1=1/3,N=1)\simeq0.63B_c(\beta_1=0,N=1)$, for all tested temperatures 304 K$\leq T_1\leq370$ K.

Now the thresholds for the case of a finite layer with $R_{\text{out}}\simeq3.33$ cm are compared. Contrary to the previous case, the threshold for a dilute fluid (dot–dashed line in Fig. 3) is lower than for a nondilute fluid (dotted line). Again the difference is almost constant over the entire temperature range, $B_c[\beta_1=1/3,N(\gamma=0.15,\chi_{\text{eff}})]\simeq1.18B_c[\beta_1=0,N(\gamma=0.15,\chi_{\text{eff}})]$.

The relation of the different thresholds is caused by the value of f_{χ_L} for the given combinations of N, β_1, and χ_L. f_{χ_L} can be considered as a measure for the strength of the magnetic force in the gap: As higher the value of f_{χ_L} as lower the critical external induction necessary to trigger the convection. Figure 5 shows the value of f_{χ_L} for the four considered parameter sets. At $\chi_L=3$ the relation $f_{\chi_L}(\beta_1=0,N=1)<f_{\chi_L}(\beta_1=1/3,N=1)$ (see cross sections of the long-dashed and the solid line with the vertical solid line) is the reason that the threshold for the dilute fluid is higher than for the nondilute fluid. The opposite relation $f_{\chi_L}[\beta_1=0,N(\gamma=0.15,\chi_{\text{eff}})]>f_{\chi_L}[\beta_1=1/3,N(\gamma=0.15,\chi_{\text{eff}})]$ (see cross sections of the dot–dashed and the dotted line with the vertical solid line) causes the opposite relation for the thresholds in the case of a finite layer.

The physical reasons which cause theses differences are the following. The Kelvin force is proportional to the magnetization in the magnetic fluid. Thus as higher the magnetization is, as lower the external induction can be in order to generate the same strength of the magnetic force. In the infinite case, where $N=1$ is independent of χ, a higher concentration of magnetic particles in the fluid leads to a higher

magnetization, and therefore, to a lower threshold. In the finite case, the demagnetization factor depends on χ[19] and is smaller for higher concentrations of magnetic particles than for lower concentrations. A higher demagnetization factor means a lower inner field and a higher magnetization, respectively. Therefore, in the finite case an increase in the concentration results in two counteracting effects with respect to the magnetization. In the studied example of $\chi_L = 3$ the influence of the demagnetization effect wins: The dilute fluid has the lower threshold. But for $\chi_L > 3.2$ the direct influence of the concentration succeeds over the demagnetization effect. The nondilute fluid has the lower threshold (the dotted line is then above the dot–dashed line, see Fig. 5).

In the infinite and finite case the clear and measurable difference between the thresholds opens a very good opportunity to decide whether a test sample is a dilute fluid or not. Just by measuring the threshold for the onset of convection in the proposed model system the answer can be given. The critical induction depends on the fluid and system parameters as $B_c \sim \kappa \sqrt{\rho}/(R_2 - R_1)$. By choosing fluids with low (high) density and thermal conductivity and a large (small) radius R_2, the threshold can be lowered (raised) corresponding to the experimentally available magnetic fields.

The major obstacle in order to compare the results with the experimental data in Ref. 10 is the lack of an experimentally determined spatial profile of the temperature inside the sample. Therefore, it is not possible to extract an estimation what might be the values of R_1 and R_2 in the experiment. Nevertheless the calculated values indicate that really high critical external inductions are necessary to trigger vertical convections rolls by a *pure radial* temperature gradient. The threshold for the induction reaches extremely high values if one extrapolates towards radii in the range of hundreds of micrometers, not unlikely due to the focused laser beam used in the experiment.[9,10] This leads to the conclusion that vertical convections rolls due to a pure radial temperature gradient are unlikely to account for the observed phenomena of polygonally shaped diffraction patterns.

Due to the lack of information from inside the sample, it is not clear whether the temperature profile in the experimental sample is purely radial. There are hints in Ref. 24 that due to the absorption along the way of the laser beam a vertical temperature distribution exists as well. A further cause for an axial temperature gradient is the heat loss through the glass plates by which the MF layer is sandwiched. If such a vertical temperature gradient comes into play, concentration gradients due to the Soret effect may become important. The relative influence of temperature and concentration gradients is strongly effected by the relation of the characteristic times t_c and t_d which depend quadratically on the lengths L_c and L_d, respectively. With a radial and a vertical temperature gradient present, it becomes even more important to have reliable data of the internal profiles to estimate these lengths.

Two differences between the model and the motivating experiment should be noted. The constant temperature T_1 for the inner cylinder is not given in the experiment. How much the temperature varies in this inner area is not known. The numerical calculations in Ref. 9 suggest a difference of about 15 K. The thresholds were calculated for rigid boundaries whereas in the experiment the fluid layer boundary is free. For thermal convection in a rotating layer of magnetic fluid the influence of rigid and free boundaries on the threshold was studied in Ref. 4. Considering the case of zero rotation, the thresholds differ by not more than 20% (see Figs. 3 and 4 in Ref. 4 for rotation number $T \rightarrow 0$). With respect to the above mentioned major obstacle, these differences may alter the results only marginally.

V. SUMMARY

A model system of a composite cylinder of finite size with axis-symmetrical temperature distribution is presented. Using the Kelvin force density (2,3) a general condition (7) is derived for which a potentially unstable stratification exists if the inner cylinder is heated. Depending on the temperature difference, the size of the composite cylinder and the dilute or nondilute character of the magnetic fluid, the critical gap sizes are calculated. The general result is that only in a narrow gap the requirement for a potentially unstable stratification is met. Exploiting this property, a linear stability analysis is performed in order to determine the critical external induction for the onset of thermomagnetic convection. With decreasing temperature difference, the critical induction increases dramatically. The reason is that for smaller temperature differences which demand smaller gaps in order to fulfill condition (7), much more convection rolls have to be driven. The driving of these many rolls causes the drastic increasing of the critical induction. The distinct difference between the threshold for dilute and nondilute magnetic fluids allows to use the considered system for an experimental determination whether a test fluid is a dilute or nondilute one.

The rather high external induction, needed to stimulate the convection flow, leads to the conclusion that vertical convections rolls due to a pure radial temperature gradient are unlikely to account for the observed diffraction patterns. The consideration of a vertical temperature gradient entails that concentration gradients may become relevant. To answer this question the characteristic time for the diffusion with respect to whose for convection has to be re-estimated. Because they will not be necessarily apart by orders of magnitude as in the case of a pure radial temperature gradient. Also different convection patterns can be expected with the presence of a vertical temperature gradient. In order to come to a correct statement about the contribution of mass and thermal diffusion to the diffraction patterns in magnetic fluids, spatial temperature measurements and independent measurements of all relevant material parameters as in Refs. 12 and 13 for an organic dispersion are highly desirable.

[1] R. E. Rosensweig, *Ferrohydrodynamics* (Cambridge University Press, Cambridge, 1985).

[2] B. A. Finlayson, "Convective instability of ferromagnetic fluids," J. Fluid Mech. **40**, 753 (1970).

[3] L. Schwab, U. Hildebrandt, and K. Stierstadt, "Magnetic Bénard convection," J. Magn. Magn. Mater. **39**, 113 (1983); L. Schwab and K. Stierstadt, "Field-induced wavevector-selection by magnetic Bénard-convection," *ibid.* **65**, 315 (1987); L. Schwab, "Thermal convection in ferrofluids under a free surface," *ibid.* **85**, 199 (1990).

[4] G. K. Auernhammer and H. R. Brand, "Thermal convection in a rotating

layer of magnetic fluid,'' Eur. Phys. J. B **16**, 157 (2000).

[5] J. Huang, B. F. Edwards, and D. D. Gray, ''Magnetic control of convection in nonconducting paramagnetic fluids,'' Phys. Rev. E **57**, R29 (1998); ''Thermoconvective instability of paramagnetic fluids in a nonuniform magnetic field,'' *ibid.* **57**, 5564 (1998).

[6] H. Morimoto, T. Maekawa, and M. Ishikawa, ''Linear stability analysis of magnetic Rayleigh–Bénard convection,'' Adv. Space Res. **22**, 1271 (1998).

[7] A. Zebib, ''Thermal convection in a magnetic fluid,'' J. Fluid Mech. **321**, 121 (1996).

[8] S. Odenbach, ''Drop tower experiments on thermomagnetic convection,'' Microgravity Sci. Technol. **VI**, 161 (1993).

[9] T. Du and W. Luo, ''Nonlinear optical effects in ferrofluids induced by temperature and concentration cross coupling,'' Appl. Phys. Lett. **72**, 272 (1998).

[10] W. Luo, T. Du, and J. Huang, ''Field-induced instabilities in a magnetic fluid,'' Phys. Rev. Lett. **82**, 4134 (1999).

[11] M. I. Shliomis and M. Souhar, ''Self-oscillatory convection caused by the Soret effect,'' Europhys. Lett. **49**, 55 (2000).

[12] W. Schaertl and C. Roos, ''Convection and thermodiffusion of colloidal gold tracers by light scattering,'' Phys. Rev. E **60**, 2020 (1999).

[13] R. Spill, W. Köhler, G. Lindenblatt, and W. Schaertl, ''Thermal diffusion and Soret feedback of gold-doped polyorganosiloxane nanospheres in toluene,'' Phys. Rev. E **62**, 8361 (2000).

[14] M. I. Shliomis, ''Comment on 'Novel convective instabilities in a magnetic fluid,''' Phys. Rev. Lett. **87**, 059801 (2001).

[15] W. Luo, T. Du, and J. Huang, ''Luo, Du, and Huang reply,'' Phys. Rev. Lett. **87**, 059802 (2001).

[16] L. Onsager, ''Electric moments of molecules in liquids,'' J. Am. Chem. Soc. **58**, 1486 (1936).

[17] M. S. Wertheim, ''Exact solution of the mean spherical model for fluids of hard spheres with permanent electric dipole moments,'' J. Chem. Phys. **55**, 4291 (1971); K. I. Morozov and A. V. Lebedev, ''The effect of magneto–dipole interactions on the magnetization curves of ferrocolloids,'' J. Magn. Magn. Mater. **85**, 51 (1990).

[18] Y. A. Buyevich and A. O. Ivanov, ''Equilibrium properties of ferrocolloids,'' Physica A **190**, 276 (1992).

[19] D. Chen, J. A. Brug, and R. B. Goldfarb, ''Demagnetizing factors for cylinders,'' IEEE Trans. Magn. **27**, 3601 (1991).

[20] A. Lange, ''Kelvin force in a layer of magnetic fluid,'' J. Magn. Magn. Mat. (to be published).

[21] T. Völker, E. Blums, and S. Odenbach, ''Thermodiffusive processes in ferrofluids,'' Magnetohydrodynamics (N.Y.) **37**, 274 (2001).

[22] S. Chandrasekhar, *Hydrodynamic and Hydromagnetic Stability* (Dover, New York, 1981), App. V.

[23] The thermal diffusivity $\kappa = \lambda/(\rho c_p)$ can only be estimated since the producer does not report the heat capacity c_p and the thermal conductivity λ of the fluid EMG 901.

[24] W. Luo, T. Du, and J. Huang, ''Field-induced instabilities in a magnetic fluid,'' J. Magn. Magn. Mater. **201**, 88 (1999).